Workshop on Visualisation in Environmental Sciences (EnvirVis) (2021)
S. Dutta, K. Feige, K. Rink, and D. Zeckzer (Editors)

# A Winding Angle Framework for Tracking and Exploring Eddy Transport in Oceanic Ensemble Simulations

A. Friederici,[1] M. Falk[2] and I. Hotz[2]

[1]Otto-von-Guericke University Magdeburg, Germany [2]Scientific Visualization Group, Linköping University, Sweden

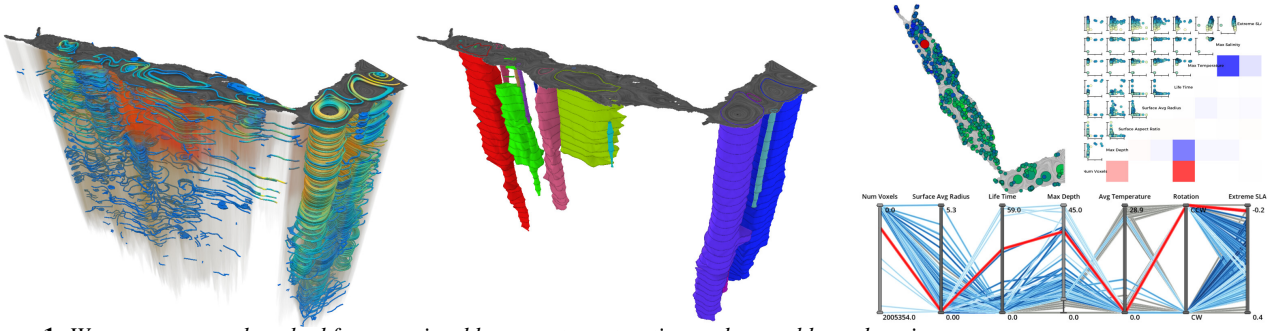


**Figure 1:** *We present a novel method for oceanic eddy geometry extraction and ensemble exploration.* ***Dataset overview*** *with streamlines and temperature volume rendering (left).* ***Eddy geometry*** *extracted using our winding angle based algorithm (center).* ***Statistics exploration*** *through multiple interactive linked views of eddy transport properties (right).*

**Abstract**

*Oceanic eddies, which are highly mass-coherent vortices traveling through the earth's waters, are of special interest for their mixing properties. Therefore, large-scale ensemble simulations are performed to approximate their possible evolution. Analyzing their development and transport behavior requires a stable extraction of both their shape and properties of water masses within. We present a framework for extracting the time series of full 3D eddy geometries based on an winding angle criterion. Our analysis tools enables users to explore the results in-depth by linking extracted volumes to extensive statistics collected across several ensemble members. The methods are showcased on an ensemble simulation of the Red Sea. We show that our extraction produces stable and coherent geometries even for highly irregular eddies in the Red Sea. These capabilities are utilized to evaluate the stability of our method with respect to variations of user-defined parameters. Feedback gathered from domain experts was very positive and indicates that our methods will be considered for newly simulated, even larger data sets.*

Categories and Subject Descriptors (according to ACM CCS): [Computer Graphics]: Human-centered computing—Scientific visualization

## 1. Introduction

The Red Sea is a marginal sea connected to the Indian Ocean via the Gulf of Aden. With its elongated and narrow basin and a low water exchange rate to the open ocean, it builds its own ecosystem. Its water circulation is largely influenced by eddies that dominate the background currents, reaching a size comparable to the width of the basin. As such they are mostly responsible for the transport of biomaterials, nutrients, and potentially pollution along and between its Arabian and African coasts [ZKGH19]. These special ecological and oceanographic conditions make Red Sea eddies especially interesting for research. Goals thereby reach from gaining a better understanding of the characteristics and evolution of eddies in the Red Sea to improving forecasting and planning [CPTV18].

Eddies are a concept describing mass-coherent bodies of swirling motion. In the open ocean, they appear close to circular, but the confines of small basins like the Red Sea can strongly deform them. The underlying simulations use numerical models of ocean dynamics, exploring parameter effects and uncertainties through large ensemble simulations [YHP*14b, YHP*14a]. The resulting data is multivariate, containing many time-dependent scalar and vector fields per ensemble member. Thus, it cannot be analyzed manually but requires a combination of automatic and inter-

Contact: anke@isg.cs.uni-magdeburg.de



DOI: 10.2312/envirvis.20211079

active analysis. This work is a refinement of our submission to the 2020 IEEE SciVis Contest. We strive to visualize and quantify eddy transport in a Red Sea ensemble simulation. We can summarize our contributions as

- Automatic explicit extraction and tracking of irregular eddies
- Quantification of the evolution of key measures
- Evaluation of the extraction algorithm using parameter studies
- Interactive analysis of all results across the ensemble

We first explore the given Red Sea data using direct visualization methods and evaluate typical vortex extraction criteria. Building on these results we design a method specifically for the Red Sea setting. This entails the extraction of explicit three-dimensional vortex regions through a winding angle criterion tracked over time, the computation of associated quantitative measures such as size and lifetime as well as statistics of transported scalars, presented through an interactive exploration framework. Overall, we received positive feedback on our extraction and visualization pipeline by the domain experts who provided the data and research questions.

## 2. Related Work

*Vortex extraction* – Vortices are not a well-defined quantity and thus their definitions and related extraction methods vary a lot. A comprehensive overview of vortex extraction methods can be found in the report by Günther et al. [GT18]. Probably one of the most prominent examples of a local vortex-identifier is the $\lambda_2$ criterion proposed by Jeong and Hussain [JH95], based on the decomposition of the velocity gradient tensor into its symmetric $S$ and antisymmetric part $\Omega$. Other related examples are vorticity, the $Q$ criterion [HWM88], and the Okubo-Weiss criterion [Oku70]. These methods are frequently used and deliver similar results. However, a fundamental problem of these methods is that they employ local operators to extract a feature spanning a large volume. As a result, these methods often detect a high number of false positives.

Non-local concepts include topological methods detecting circular critical points [HH90] or closed streamlines in a 2D flow [WSH01, TWHS04]. Other methods are based on integral line geometry. The method by Sadarjoen and Post [SP00] utilizes the integrated winding angle to find almost closed streamlines. Petz et al. [PKPH09] define hierarchical vortex regions in swirling flows as being enclosed by streamlines of a locally rotated flow field. There exist also methods based on observations that vortices represent coherent motions which tend to maintain a relatively constant set of particles. For example, Froyland et al. [FHRvS15] apply coherent sets to extract eddies in 2D flows. Several other methods consider coherence using the concept of the Finite-Time Lyapunov Exponent (FTLE) based on Haller's work [Hal00], among others for ocean eddy extraction [BVOG08]. The downside is their high computational cost, which is not feasible in our ensemble case.

*Ocean eddy visualization and analysis* – Eddies can be considered a special kind of vortices, so all vortex extraction methods can be applied, though not all with satisfying results. An overview with applications in oceanographic and atmospheric sciences has been presented by Afzal et al. [AHG*19]. Often, data stems from numerical simulations and data from satellite imaging [CPTV18], including sea surface temperature (SST) or sea level anomaly (SLA) that contains valuable information about oceanic eddy characteristics. Dong et al. [DNYL11] propose an automated eddy detection scheme pinpointing minima in the surface velocity field as eddy center points with contours of the SST fields as boundaries. Zhan et al [ZSYH14] define surface-based eddy centers located at local extrema of the SLA field. The outer-most closed streamlines thats surrounds the eddy center is identified via a winding angle criterion characterize the eddy boundary. Variants relax the criterion even further to allow coast-bound eddies [ZKGH19]. They are tracked through distance-based correspondence. Similar to this approach, we build on the winding-angle criterion to generate eddy boundary candidates while both extending it to three dimensions and allowing smaller boundary candidates for a smoother final surface. We also base our method on the streamlines alone, sampling the domain densely to find all potential eddies even in lower depths.

Of the standard vortex extraction methods, the Okubo-Weiss criterion can frequently be seen in this application domain, though it has been shown to not always give accurate results [CGG08]. Williams et al. [WHP*11, WPH*12] filter out the high number of false positives with a circularity criterion.

A number of works investigate eddies in the context of Lagrangian coherent structures (LCS) using FTLE on surface ocean currents [HP97, ACSZS13]. Harrison and Glatzmaier [HG12] express the limitations of LCS methods in a study which show the high sensitivity of high shear regions that are not part of the eddy. Friederici et al. [FKH*18] applied a 2D Lagrangian method on Red Sea eddies focusing on mass conservation over time. Most of the methods mentioned are limited to two dimensions, and their high computational cost renders them impractical for ensemble data.

*Multi-field and ensemble visualization* – In this works, we visualize ensemble data from multiple simulations runs sampling a large parameter space, here uncertain initial conditions, which also containing multiple vector and scalar fields. This is a challenging setting treated by a lot of previous work summarized in a survey by Wang et al. [WHLS18]. Claessen and van Wijk [CvW11] summarize the high-level interest in multivariate data visualization as showing individual items, showing the distribution of values for a single attribute, and the correlation between values for two attributes. In this respect, probably the most popular visualizations are scatterplots, scatterplot matrices, and parallel coordinates plots [ID90], which also provide good interfaces for interactive exploration and filtering of multivariate data [BC87]. We offer several such linked visualizations on top of our eddy extraction.

## 3. Red Sea Dataset

In this work, we use the Red Sea dataset which was provided for the 2020 IEEE VIS SciVis contest. The dataset covers the entire Red Sea up to the Gulf of Aden, which is prominently shown in Figure 1. It consists of 50 ensemble members, each describing a domain of $500 \times 500$ cells horizontally with a 4 km spacing, 50 cells of increasing depth, and 60 time steps over one month. A large-scale simulation based on ensemble data assimilation was used to create the individual ensemble members [TZG*17]. The given data includes both velocity and scalars covering salinity, temperature (Figure 1, left), surface level anomaly (SLA) and is available at `https://kaust-vislab.github.io/SciVis2020/`.

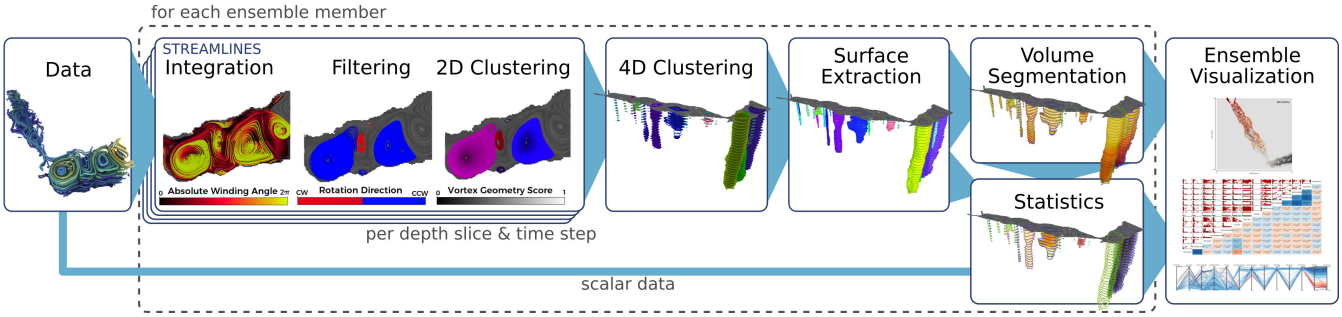


**Figure 2:** *Overview of our method. For each ensemble of the input data, streamlines are computed and clustered for all depth slices and time steps. We then cluster the result over all time steps and extract optimal surfaces. These are then used to apply a volume segmentation and to gather statistics of the eddies. Finally, the collected ensemble data can be explored and analyzed interactively.*

### 3.1. General Considerations for the Method Design

When searching for eddies, several vertex extraction methods are available [GT18]. However, the particular conditions of the Red Sea's confined basin challenge many of these methods. For a better understanding of the dataset characteristics we studied selected ensemble members using the visualization software *Inviwo* [JSS*19].

We started with investigating typical scalar vortex identifiers: vorticity, vector field curvature, $\lambda_2$, and the Okubo-Weiss criterion, see Figure 3. All these methods are successful in detecting the major eddies in the Gulf of Aden, however, they generate a lot of false positives when applied to the Red Sea especially close to the coast due to shear. In a second step, we analyzed and compared standard streamline and pathline visualizations. While the pathlines diverge from the streamlines over time, streamlines provide a good approximation of developing structures. As is common in oceanic flow, the horizontal transport is two orders of magnitude larger than the vertical transport (compare Figure 1 left). Eddies are thus composed of almost horizontal slices of swirling movement. In conclusion, this resulted in the decision to use an Eulerian streamline-based method that composes the eddies from a slice-based analysis.

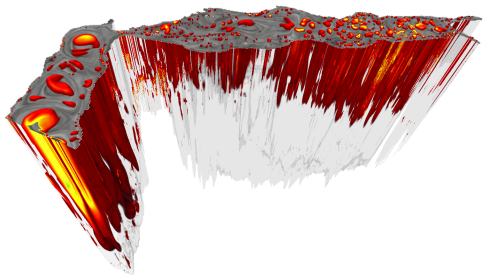

**Figure 3:** ***Okubo-Weiss:*** *we computed the Okubo-Weiss criterion, rendering eddy regions in red. Yellow marks more extreme values. Though the large eddies in the Gulf of Aden to the left are somewhat recognizable, the Red Sea itself is cluttered with false-positives.*

## 4. Our Approach

Two streamline-based methods that have been proposed previously are especially suitable for this situation. This is the method by Sadarjoen et al. [SP00] using the integrated winding angle and the approach by Petz et al. [PKPH09] who define hierarchical vortex regions in swirling flow, which are enclosed by streamlines of a rotated flow field. Due to its conceptual simplicity and clear eddy streamline geometry observed, we chose the first of these methods. The basic idea of the method is to search for *almost closed streamlines* and thus relaxing the criterion for a closed circle. The *winding angle criterion* only requires the line to exceed an accumulated turning angle of $2\pi$, and an endpoint close to its origin. An eddy contains many such nested lines. Disregarding vertical transport, we can view an eddy as a stack of almost closed streamlines reaching from the surface into the depth, see Figure 4. From the resulting streamline candidates we extract explicit closed surfaces and obtain our 4D space-time eddies, see Figures 5-6. These enable a quantitative analysis of transport. For each eddy, we derive a set of key measures including lifetime, mass, temperature, salinity, and surface-level anomaly both per time step and as a time series. The resulting statistical measures are then represented in statistical plots which are linked to the 3D geometry visualization, providing an integrated view of geometry and transport. The measures are also used for filtering and the inspection of the temporal evolution of selected eddies. Examples of the tool in action are provided in the supplemental video. All implementations are available open source as external modules of the Inviwo visualization software [JSS*19].

### 4.1. Eddy Extraction Pipeline

In the following, we describe the individual parts of our algorithm for a full boundary extraction within a single ensemble member as illustrated in Figure 2.

**Streamline Integration –** The first step is to generate streamlines which will serve as input for subsequent steps. Given a single horizontal 2D slice of the vector field, we densely seed streamlines across the whole domain. During integration, the winding angle is accumulated as the sum of the signed angles between samples. At $\pm 2\pi$, the integration is terminated. A set of such lines on the surface of the Gulf of Aden is shown in Figure 2 as "Integration".

**Streamline Filtering –** A high winding angle does not necessarily mark a streamline as almost closed. We filter lines by a maximal distance between the line's start and endpoint relative to the streamline's length and the approximate aspect ratio of the shape. This discards exceedingly non-circular shapes early in the pipeline

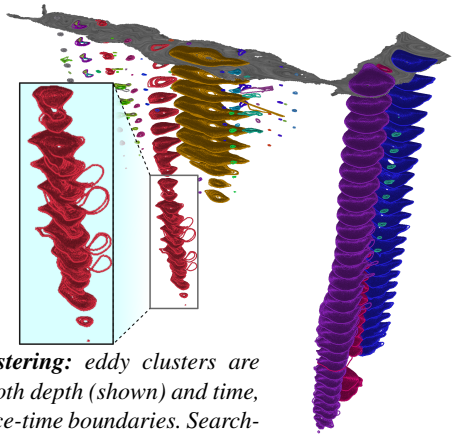

**Figure 4:** ***4D clustering:*** *eddy clusters are connected across both depth (shown) and time, resulting in 4D space-time boundaries. Searching is seeded close to the surface and matches based on position and average radius.*

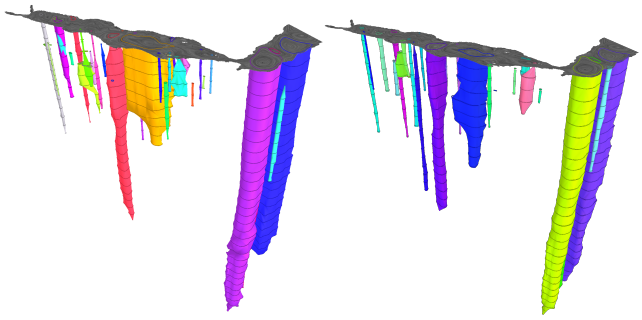

**Figure 5:** ***Optimal surface extraction:*** *optimal boundaries are chosen per depth and time slice and connected to a surface. The optimum is found as a combination size, roundness and similarity between slices. The right result was additionally restricted to an absolute winding angle of* $3\pi$ *to limit concavity.*

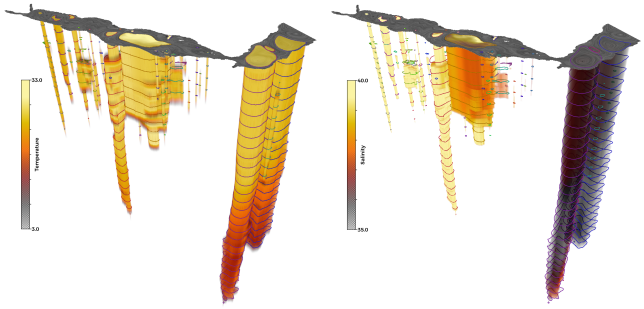

**Figure 6:** ***Ensemble statistics:*** *the final step in our pipeline gathers the statistics over all ensembles by masking the scalar volumes with the extracted eddies. Here, temperature and salinity inside the eddies are visualized as a volume rendering.*

(see Figure 2, "Filtering"). The distance and shape parameter will be further explored in Section 6.2. A center is assigned to each streamline as the barycenter of all line points.

**2D Streamline Clustering –** To find a single representative streamline that serves as eddy boundary, we first identify clusters as lines including each others center points, shown in Figure 2 "2D Clustering". Then, we rank the streamlines according to their size and roundness, respectively. The idea behind this is to assign a score that favors lines which better enclose the full eddy mass, while at the same time excludes strongly deformed shapes. See for example the red eddy in Figure 4 at lower depths. The roundness value is computed as the ratio between the maximal and minimal radius. For finding a balance between these scores, we combine them as a weighted sum. The impact of this weight parameter on the results is demonstrated in Section 6.2. In further collaboration with domain experts other heuristics could be implemented easily, such as the convexity criterion proposed (see Section 6.3 and Figure 5, right).

**4D Clustering –** As the 2D clusters are computed for each depth slice and time step, we construct spatio-temporal 4D line sets per eddy according to their center point location(Figure 4). We seed this search at an eddy's first appearance close to the surface and then propagate in depth and over time. Since eddies are surface vortices, line clusters not connected to the surface are discarded. We found several such vortices quite commonly located at the bottom of the Gulf of Aden which might warrant further investigation. Our approach does not support the splitting and merging of vortices.

**Optimal Surface Extraction –** In the last step, a closed boundary surface is generated. Within each cluster of concentric lines, a representative boundary is chosen by a combination of the vortex score (which is itself based on the size and aspect ratio of the shape) and the similarity to its neighbors in both time and space. All eddy selection heuristics can be adapted interactively when exploring one ensemble member. The streamlines are closed by connecting start and endpoint and smoothing out a short section at the end. We then create a smooth loft surface by connecting neighboring boundary curves. This closed surface represents the eddy through space and time, seen for one time step in Figures 1, center and Figure 5.

**Ensemble Statistics Generation –** In order to explore the transport of tracer quantities, here salinity and temperature, we require a full volumetric representation of the extracted eddies. We achieve this efficiently by rendering the 2D boundaries as triangle fans slice-wise into a volume texture and utilizing GPU rasterization capabilities. Given this volume, we mask the underlying scalar volumes of the dataset and gather statistics on each eddy's average, minimal and maximal temperature respective salinity. These values are recorded both per time slice and per ensemble, a volume rendering of which can be seen in Figure 6. In addition, we store quantities directly given by the boundary geometry, namely the average radius and aspect ratio at the surface, depth reached, start and end positions, traveled distance, and overall lifetime of the eddy.

The full extraction pipeline computes in 35 minutes per ensemble member (30GB, 8 million streamlines) on a single thread of an Intel i9 CPU at 2.40GHz and can thus easily be parallelized. The visualization runs independently on saved eddy results.

### 4.2. Visual Exploration

The resulting statistics are used to explore the entire ensemble. They provide a summary of the geometric and physical measures

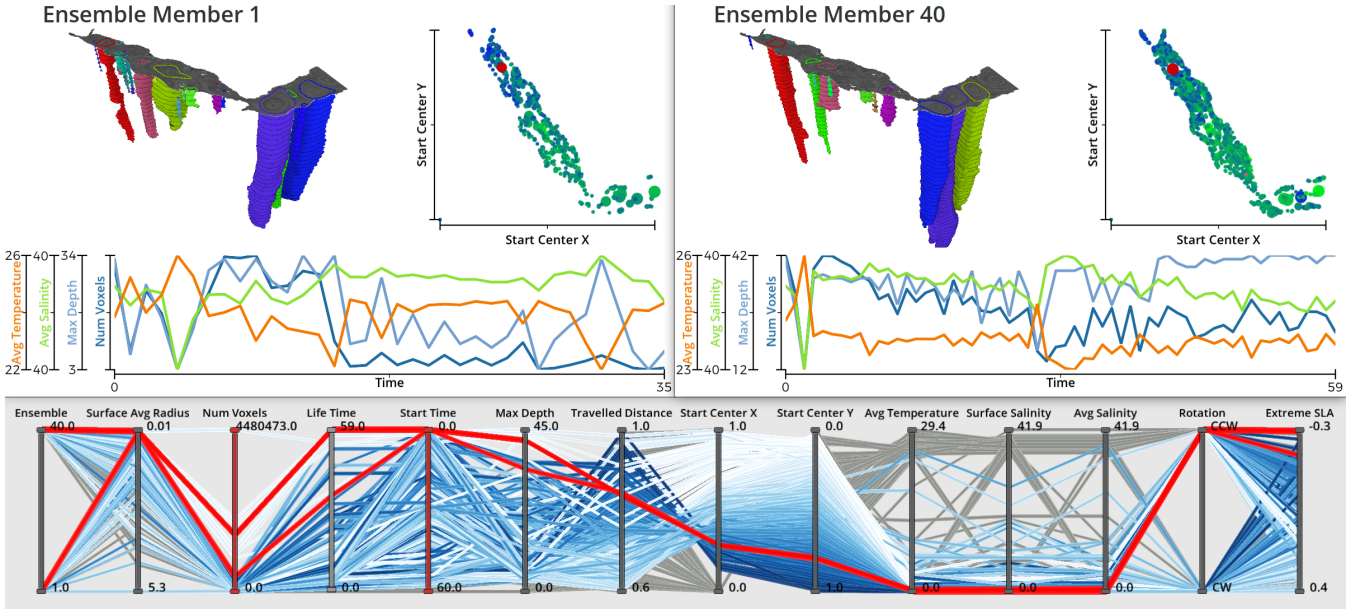


**Figure 7:** ***Transport statistics comparison between members:*** *we enable the users to filter the extracted eddies, such as by size, roundness or lifetimes, and to analyze their correlations. To this end, we provide several views: the rendering of the eddy geometry gives the best idea of an eddy's shape and location. A spatial scatterplot contains all eddy locations, with depth mapped to size and surface level anomaly to color. Below, graphs of transport properties lay out the time axis. Parallel coordinates provide an overview of all eddies and allow for simple filtering. All views are fully linked. Here, similar eddies were selected manual (red). Please refer to the additional video for an in-depth view.*

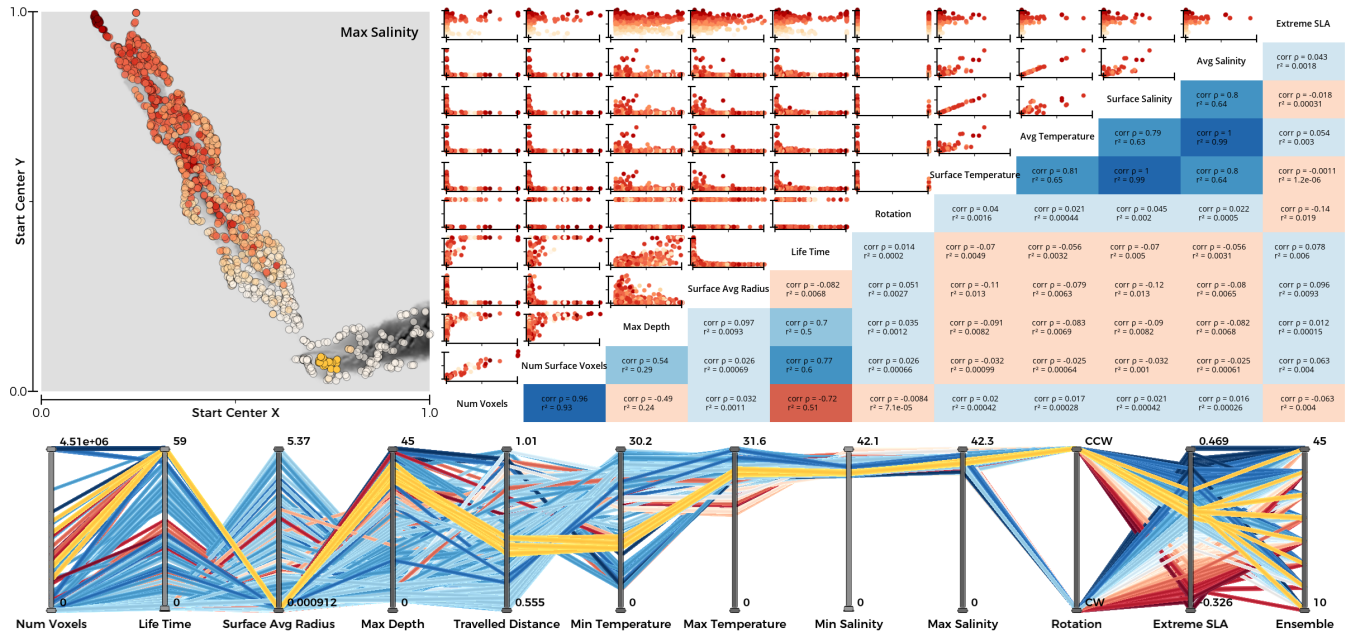


**Figure 8:** ***Evaluation of ensemble statistics:*** *combining the statistics of several ensemble members, we can visually explore the overarching distributions across the data. Here, eddies from eight different members are compared against each other. A large scatterplot matrix enables a statistical evaluation . Most notably, temperature and salinity are strongly correlated. In the parallel coordinates view, eddies are filtered out based on their lifetime. A spatial scatterplot shows the distribution of the remaining eddies across all members. By selecting all eddies in the orange region, we can explore their properties across members. They are remarkably similar, with exactly one eddy per member.*

of all eddies over all ensembles. Available statistical views include timeline plots representing the evolution of parameters of selected eddies. Other plots like parallel coordinates, scatterplots, and corresponding correlation plots provide the possibility to explore relationships between parameters and/or eddies within or across ensemble members (Figure 1, right). Spatial representations can be chosen to display three-dimensional eddies in a selected ensemble at a selected time, or for a selected depth across time. An alternative rendering are two-dimensional slice views in which aggregated properties of all ensemble members are shown simultaneously for side-by-side comparisons. All views are connected via bushing and linking providing a smooth exploration framework (Figure 8).

## 5. Results

Our work was motivated by the IEEE SciVis Contest 2020. The visualization community was asked to contribute tools for an evaluation of eddy transport. To this end, we provide two interactive visualizations which we explore further in the accompanying video.

**Eddy Property Exploration –** The first contest tasks asked participants to visualize transport properties of Red Sea eddies. We allow the user to explore the distribution of eddies, differences between ensemble members, and the correlation of all collected properties. Figure 7 shows a view to compare ensemble members against each other in-depth, including their geometry, spatial distribution, and time plots of selected features. A parallel coordinates view of most gathered properties including both member's data links them together. All sections are connected to allow for brushing and linking. In this example, we selected the eddy in the north of the Red Sea in both members 1 and 40. We can observe their difference in geometric shape and lifetime across views. However, the parallel coordinates plot reveals a strong similarity in all other properties.

**Ensemble Statistics Exploration –** A main question concerns the statistical evaluation of eddy transport within the whole ensemble. To this end, we provide a second visualization tool targeted at comparing large amounts of eddies (see Figure 8). At more than 6000 individual eddies, filtering becomes crucial, here to remove short-lived eddies. One interesting feature to observe across members is the semi-stable eddy at the touching point of the Red Sea and the Gulf of Aden. We selected this region in the spatial scatter plot overview, showing a strong similarity between all instances. Notably, exactly one eddy is present in this region per member. A main question of the contest was the correlation between temperature and salinity across the whole ensemble. The scatter plot matrix shows their strong correlation, marked by a block of dark blue correlation values and strong trends in the corresponding scatter plots, in addition to several other properties. Other relationships can be observed in this view, such as eddies with a large surface area reaching deeper. All views presented in these two visualizations can easily be combined and extended to answer further questions.

## 6. Evaluation

In this section, we describe the evaluation of our proposed method with respect to the basic observations stated in Section 3.1, the dependence of the results on the algorithmic parameters and feedback received by the domain experts.

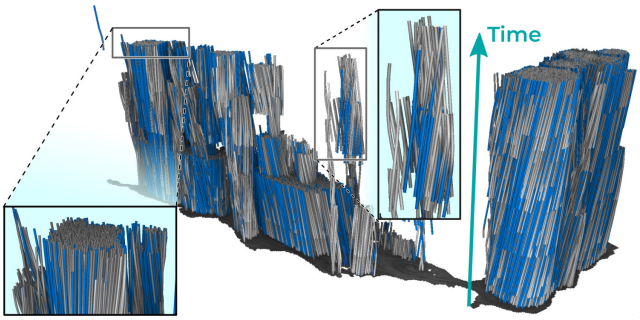


**Figure 9:** ***Mass coherence computation:*** *from random samples within the extracted eddy regions, pathlines are integrated forwards and backwards in time. The vertical, third dimension corresponds to time over 2.5 days (5 time steps). Integration time is shown in grayscale. Where particles leave their eddy's boundary, they are highlighted in blue. Two regions are highlighted: in large eddies, only a small percentage of particles escape the boundary. But we can also observe smaller, yet stable regions.*

### 6.1. Coherence Computation

An important measure of the stability of an extracted eddy is its mass coherence, capturing how much water remains within the boundaries of the eddy in subsequent time steps. To quantify this measure, we trace particles randomly seeded within the volumes of all eddies. Integrating both forward and backward one time step, we measure the percentage of particles that remain within the eddies' enclosure. A high value here means that we neither overestimate nor underestimate an eddy's volume, but have successfully identified a stable body of water. Figure 9 depicts the results of such a mass coherence computation where only a small percentage of mass is lost over time, thus indicating rather stable eddies.

To compress these measures into a single number for a given eddy segmentation, we provide two options: simply average the coherence of all voxels integrated from, or calculate an average per-eddy coherence. Since mass escapes the eddy at the boundaries only and the ratio of volume to surface increases roughly linearly with radius, the former measure favors eddies of large volume. All together, mass coherence provides us with a simple measure of stability to judge the overall quality of the eddies and their boundaries.

### 6.2. Parameter Study

We purposefully left a number of computation parameters exposed so that users can apply their knowledge. However, we could easily find settings that produced consistent results across ensemble members. In Figure 10, we show the influence of these parameters on the resulting geometry. One interesting indicator is the volume and surface area of the largest eddy, located in the middle of the Red Sea. In addition, the two coherence measures described above are included as well as the total number of eddies over a short time.

**Endpoint Distance –** Our eddy extraction pipeline builds on top of the winding angle method: from densely seeded streamlines fulfilling a circle, consider all that end within a small distance to their seed point. We set this maximal distance relative to the streamline's length, thus considering the geometry only, irrespective of size.

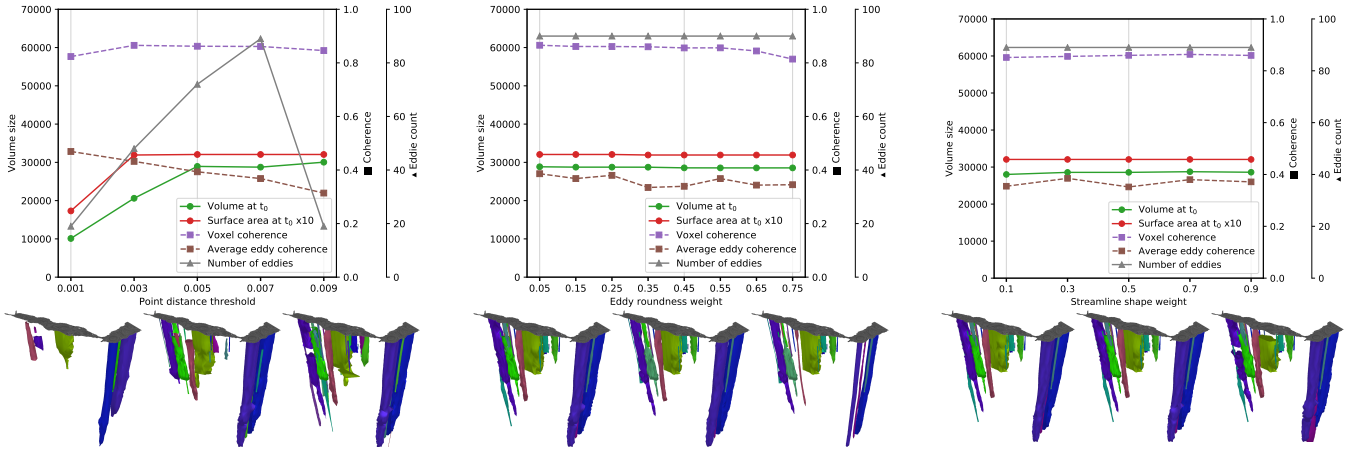


**Figure 10:** ***Parameter study:*** *we plot the influence of three parameters controlling the eddy surface extraction, namely point distance threshold (left), the weight of eddy roundness against its size (center), and the influence of this combined measure against the size difference between slices (right). They manifest in the total number of eddies across the time series, the volume change of the largest eddy (dull green in the middle of the Red Sea), and the overall coherence for variations of those values. The visualizations below correspond to the parameters indicated by the gray vertical lines in each plot (left-most, center, right-most parameters, respectively).*

The effect of this relative threshold on the geometric result is shown in Figure 10, left. For an increasing parameter, less closed and thus generally less round streamlines are kept, as can be seen in the three extracted geometries below. After a certain point shapes start to degenerate (see rendering for threshold at 0.009). At that point, the higher number of streamlines to select from enables our pipeline to trace eddies for longer, resulting in less eddies. To find a balance between low stability and a low number of eddies, we have found all parameters in the mid-range to work well, employing a relative endpoint distance threshold of 0.07 throughout this work.

**Clustering Weights –** Our surface extraction step requires us to rate eddy boundary candidates such that an optimal 4D geometry can be found. It consists of three parts: the roundness of a candidate given by its aspect ratio, the candidate's size favoring larger radii, and the size difference to the neighboring depth and time slices. We analyzed the influence of favoring roundness over size. All indicator values remain stable, while we can see changes in the renderings where the radii of most eddies shrink to rounder streamlines in the center of eddies. Generally, this choice is up to the user.

The last parameter within our pipeline is the weight between a candidate's score in contrast to the size difference with the last selected boundary line. Overall, this choice produces very similar results as the slow flow produces similar line sets across both depth and time. Only in the last rendering do we see deformations in the Gulf of Aden's eddies. We expect this parameter to play a more significant role in less stable datasets and lower time resolutions.

### 6.3. Domain Expert Feedback

We presented our pipeline and results to the domain scientists of the King Abdullah University of Science and Technology (KAUST) who posed the IEEE SciVis Contest 2020. Our eddy extraction pipeline is similar to methods they employ themselves and filters eddy candidates with similar criteria. They proposed a fixed range of 50-200 km for eddy radii and putting more emphasis on similarity in size when establishing the optimal boundary surface. These weights can easily be set. In addition, they suggested an additional boundary selection criterion based on the sum of absolute angles inscribed as a measure of convexity. Figure 5 shows an example with this filter applied, leading to generally rounder shapes.

We explained the parallel coordinates plot and scatter plot matrix in detail to the domain scientists, who where not familiar with these types of plots. The linked parallel coordinates view (see figure 8 and 7) offered them an immediate compact view of their data, an overview of the eddy distributions and simple interactive filtering. The experts would like to apply our tools to larger data sets, making use of the fact that the eddy extraction can be computed offline to allow for an interactive analysis.

## 7. Conclusion

In this work, we presented a framework for the automatic extraction and exploration of eddies in the Red Sea and the Gulf of Aden. The proposed algorithm is based on a simple 2D slice-based algorithm for assembling 4D space-time eddies. Despite the simplicity of the approach, it outperforms many of the popular vortex extraction methods based on local scalar identifiers. Due to the explicit extraction of a space-time boundary, it supports the automatic extraction of key eddy measures allowing for ensemble comparisons.

A limiting factors of the algorithm are the involved parameters, which influence quantitative measures. A parameter study showed that the impact is not severe. However, a more in-depth analysis of the results by domain scientists might be necessary. To keep the method transparent, all parameters are exposed to the user and allow interactive adaptation. However, for the exploration of the ensemble this is not feasible anymore and one fixed set of parameters has to be chosen for an offline extraction of all statistical measures.

We evaluated the algorithm with respect to mass conservation, a measure that has also been used to define eddies. The results were satisfactory, however, the used coherence measure might not be the optimal choice since it biases either eddy count or size. To further explore the impact of parameter sets defining the simulations it would be interesting to include these into the analysis pipeline. Especially a sensitivity analysis would help improve future parameter choices. In addition, a clustering of the ensemble members with respect to characteristic feature vectors could be advantageous.

## Acknowledgments

This work was supported through grants from the Excellence Center at Linköping and Lund in Information Technology (ELLIIT), the Swedish e-Science Research Centre (SeRC), and a grant from the Swedish Foundation for Strategic Research (SSF, BD15-0082). The Red Sea data is courtesy of the Red Sea Modeling and Prediction Group. We wish to thank Ibrahim Hoteit, Peng Zhan and Tom Theussl for taking the time to provide feedback on our work.

## References

[ACSZS13] ANDRADE-CANTO F., SHEINBAUM J., ZAVALA SANSÓN L.: A lagrangian approach to the loop current eddy separation. *Nonlinear Processes in Geophysics 20*, 1 (2013). 2

[AHG*19] AFZAL S., HITTAWE M., GHANI S., JAMIL T., KNIO O., HADWIGER M., HOTEIT I.: The state of the art in visual analysis approaches for ocean and atmospheric datasets. *Computer Graphics Forum 38*, 3 (2019). 2

[BC87] BECKER R., CLEVELAND W.: Brushing scatterplots. *Technometric 28*, 2 (1987). 2

[BVOG08] BERON-VERA F. J., OLASCOAGA M. J., GONI G. J.: Oceanic mesoscale eddies as revealed by Lagrangian coherent structures. *Geophysical Research Letters 35*, 12 (2008). 2

[CGG08] CHAIGNEAU A., GIZOLME A., GRADOS C.: Mesoscale eddies off Peru in altimeter records: Identification algorithms and eddy spatio-temporal patterns. *Progress in Oceanography 79*, 2 (2008). 2

[CPTV18] CHASSIGNET E. P., PASCUAL A., TINTORE J., VERRON J. (Eds.): *Data Assimilation in Oceanography: Current Status and New Directions*. 2018. 1, 2

[CvW11] CLAESSEN J. H., VAN WIJK J. J.: Flexible linked axes for multivariate data visualizations. *Transactions on Computer Graphics and Visualization 17*, 12 (2011). 2

[DNYL11] DONG C., NENCIOLI F., Y. LIU A. J. C. M.: An automated approach to detect oceanic eddies from satellite remotely sensed sea surface temperature data. *IEEE Geoscience and Remote Sensing Letters 8*, 6 (2011). 2

[FHRvS15] FROYLAND G., HORENKAMP C., ROSSI V., VAN SEBILLE E.: Studying an Agulhas ring's long-term pathway and decay with finite-time coherent sets. *Chaos: An Interdisciplinary Journal of Nonlinear Science 25*, 8 (2015). 2

[FKH*18] FRIEDERICI A., KELE H. T. M., HOTEIT I., WEINKAUF T., THEISEL H., HADWIGER M.: A Lagrangian method for extracting eddy boundaries in the Red Sea and the Gulf of Aden. In *IEEE Scientific Visualization Conference* (2018). 2

[GT18] GÜNTHER T., THEISEL H.: The state of the art in vortex extraction. *Computer Graphics Forum 37*, 6 (2018). 2, 3

[Hal00] HALLER G.: Finding finite-time invariant manifolds in two-dimensional velocity fields. *Chaos 10* (2000). 2

[HG12] HARRISON C. S., GLATZMAIER G. A.: Lagrangian coherent structures in the California current system–sensitivities and limitations. *Geophysical & Astrophysical Fluid Dynamics 106*, 1 (2012). 2

[HH90] HELMAN J., HESSELINK L.: Representation and display of vector field topology in fluid flow data sets. *Visualization in Scientific Computing* (1990). 2

[HP97] HALLER G., POJE A.: Eddy growth and mixing in mesoscale oceanographic flows. *Nonlinear Processes in Geophysics 4* (1997). 2

[HWM88] HUNT J. C., WRAY A., MOIN P.: Eddies, streams, and convergence zones in turbulent flows. In *Studying Turbulence Using Numerical Simulation Databases* (1988), vol. 2. 2

[ID90] INSELBERG A., DIMSDALE B.: Parallel coordinates: A tool for visualizing mult-dimensional geometry. In *IEEE Visualization Conference* (1990). 2

[JH95] JEONG J., HUSSAIN F.: On the identification of a vortex. *Journal of fluid mechanics 285* (1995). 2

[JSS*19] JÖNSSON D., STENETEG P., SUNDÉN E., ENGLUND R., KOTTRAVEL S., FALK M., YNNERMAN A., HOTZ I., ROPINSKI T.: Inviwo - a visualization system with usage abstraction levels. *IEEE Transactions on Visualization and Computer Graphics (TVCG)* (2019). 3

[Oku70] OKUBO A.: Horizontal dispersion of floatable particles in the vicinity of velocity singularities such as convergences. In *Deep Sea Research and Oceanographic Abstracts* (1970), vol. 17. 2

[PKPH09] PETZ C., KASTEN J., PROHASKA S., HEGE H.-C.: Hierarchical vortex regions in swirling flow. *Computer Graphics Forum 28*, 3 (2009). 2, 3

[SP00] SADARJOEN I. A., POST F. H.: Detection, quantification, and tracking of vortices using streamline geometry. *Computers and Graphics 24*, 3 (2000). 2, 3

[TWHS04] THEISEL H., WEINKAUF T., HEGE H.-C., SEIDEL H.-P.: Grid-independent detection of closed stream lines in 2D vector fields. In *VMV* (2004), vol. 4. 2

[TZG*17] TOYE H., ZHAN P., GOPALAKRISHNAN G., KARTADIKARIA A. R., HUANG H., KNIO O., HOTEIT I.: Ensemble data assimilation in the Red Sea: Sensitivity to ensemble selection and atmospheric forcing. *Ocean Dynamics 67*, 7 (2017). 2

[WHLS18] WANG J., HAZARIKA S., LI C., SHEN H.-W.: Visualization and visual analysis of ensemble data: A survey. *IEEE Transactions on Visualization and Computer Graphics* (2018). 2

[WHP*11] WILLIAMS S., HECHT M., PETERSEN M., STRELITZ R., MALTRUD M., AHRENS J., HLAWITSCHKA M., HAMANN B.: Visualization and analysis of eddies in a global ocean simulation. *Computer Graphics Forum 30*, 3 (2011). 2

[WPH*12] WILLIAMS S., PETERSEN M., HECHT M., MALTRUD M., PATCHETT J., AHRENS J., HAMANN B.: Interface exchange as an indicator for eddy heat transport. *Computer Graphics Forum 31*, 3 (2012). 2

[WSH01] WISCHGOLL T., SCHEUERMANN G., HAGEN H.: Tracking closed streamlines in time dependent planar flows. In *VMV* (2001). 2

[YHP*14a] YAO F., HOTEIT I., PRATT L. J., BOWER A. S., KÖHL A., GOPALAKRISHNAN G., RIVAS D.: Seasonal overturning circulation in the red sea: 2. winter circulation. *Journal of Geophysical Research: Oceans 119*, 4 (2014). 1

[YHP*14b] YAO F., HOTEIT I., PRATT L. J., BOWER A. S., ZHAI P., KÖHL A., GOPALAKRISHNAN G.: Seasonal overturning circulation in the Red Sea: 1. Model validation and summer circulation. *Journal of Geophysical Research: Oceans 119*, 4 (2014). 1

[ZKGH19] ZHAN P., KROKOS G., GUA D., HOTEIT I.: Tree-dimensional signature of the Red Sea eddies and eddy-induced transport. *Geophysical Research Letters* (2019). 1, 2

[ZSYH14] ZHAN P., SUBRAMANIAN A. C., YAO F., HOTEIT I.: Eddies in the Red Sea: A statistical and dynamical study. *Journal of Geophysical Research: Oceans 119*, 6 (2014). 2